Assessing Geohazard Impact on Buried Pipeline Integrity via Critical Strain-Based Failure Model

Shree Krishna, Udayasankar Arumugam, Ryan Milligan, Ravi Krishnamurthy
Blade Energy Partners

Organized by
CLARION
TECHNICAL CONFERENCES

https://doi.org/10.52202/078572-0019

https://doi.org/10.52202/078572-0019

Abstract

This paper introduces a methodology aimed at analyzing failures in buried pipelines exposed to significant geotechnical displacement. The occurrence of ground movement and heave generates substantial longitudinal strain through elongation and bending, potentially leading to buckling in the pipeline segment. Buckling, in turn, can compromise the pipeline's elastic stability, allowing further elongation with soil movement. The girth weld's presence acts as a potential weak point, susceptible to either brittle or ductile failure. Conventional analyses using standards such as ASME B31.8 or API 1104 tend to provide conservative estimations and often fail to fully elucidate the extent of geotechnical displacement or the root cause of failures. Moreover, these approaches overlook addressing failures that may occur when the girth welds are ductile in nature as specified in API 1104. This is especially true for modern steels.

To effectively tackle extensive geotechnical displacement, this paper advocates strain-based damage methodologies utilizing critical strain as a pivotal material parameter. Understanding the true stress-strain behavior, particularly the critical strain parameter of base metal, Heat Affected Zone (HAZ), and weld, is crucial in predicting potential failure. The paper's approach involves reviewing existing strain-based failure methodologies in literature and then delving into analyzing the geotechnical movement of buried pipeline segments using a critical strain-based failure criterion. The lateral displacement of the pipeline is analyzed through a finite element approach that integrates both global and detailed local sub-modeling. This examination includes showcasing the impact of weld misorientation and the presence of planar defects related to welding. The paper also discusses the evolution of damage at the local girth weld, emphasizing the significance of the "Ductile Failure Damage Indicator (DFDI)" parameter. Finally, a series of finite element analyses illustrate the loss of elastic stability due to buckling in pipes subjected to pure bending and internal pressure. It concludes by outlining the limitations of other geohazard fitness-for-purpose approaches relying on parameters like CTOD (Crack Tip Opening Displacement) and demonstrates the successful application of the methodology in analyzing a buried pipeline failure.

INTRODUCTION

A logical pathway for addressing geohazards (i.e., heavy rainfall mudslides, progressive slope movements, earthquakes etc.) would be to determine the nature of the strain demand caused by the geohazards. This could involve assessing the potential for ground settlement/movement leading to pipe-soil interaction, thereby introducing substantial axial, and bending strains on the pipeline. This strain demand may be a one-time event or accumulative over a service period of the pipeline. Once the nature of the strain demand (tensile or compressive) is determined, further steps can be taken to evaluate the strain capacity and develop appropriate design and mitigation measures to address the geohazards. The strain capacity of the pipeline is the strain limit beyond which the pipe would experience a drop in load carrying ability or material failure. The strain capacity of the pipeline will

https://doi.org/10.52202/078572-0019

be completely justified, only if we know the material characteristics of the pie material, for example the yield strength, elongation, ductility, and fracture toughness.

The strain capacity of the pipeline would depend on the main failure modes or the limit states that are associated with the material characteristics and the presence of defects if any. With the absence of defects, it can be stated that the pipeline can sustain large geotechnical displacements. Further Engineering Critical Assessments (ECA) can be conducted to determine acceptable flaw sizes in pipeline girth welds that can sustain the strain demand. Recent paper by Wang and Wu [1] reviewed all the existing strain capacity models used by pipeline community. A number of fracture mechanics-based procedures are available for ECA of pipeline girth welds. Most of these methods are primarily stress based assessments and are therefore not directly applicable to cases where the displacement-/strain-controlled loading generates large amounts of plastic deformation. For such cases, strain-based fracture assessment for pipeline/girth welds should be carried out instead.

CSA Z662-23 [2] incorporates a strain capacity that does not depend on the strain hardening material characteristics or distinguish between the pipe material or weld material. Exxon-Mobil methodology [3] developed over 15 years and using 50 full scale tests outlines an approach for strain-based design approaches. PRCI-CRES [4, 5, 6] models are also prevalent outlining the tensile and compressive stain capacity of the pipeline. However, all these models require a crack-like flaw assumption. The fracture-mechanics based approaches [7] require a stationary crack model that doesn't reflect an undamaged ductile material scenario. All these models currently predict a strain capacity of around 6-7% for a small flaw size. This prediction is conservative, based on the true strains observed in many large displacement failures.

There are no appropriate strain-based methods [1, 8, 9] available for the assessment of the pipelines subjected to large plastic straining with and without internal pressure. In addition, the girth weld geometry, weld material characteristics and associated anomalies should be uniquely accounted for in predicting the strain for failure. Damage mechanics model from ExxonMobil [7] tends to predict the strain capacity with an inherent flaw assumption and requires more than 44 parameters. In addition, models [7] consider a strength overmatch of weld material curves, which doesn't reflect the actual ductility of the weld or HAZ materials. Also, the synergistic effect of buckling followed by large deformation rupture in overall failure mechanism should be captured for the failure event. Therefore, a more physics-based strain damage approach capturing the ductility and the material characteristics should be developed and brought forward for the strain-based assessment of pipelines.

This paper presents a unique application of the critical strain-based ductile damage methodology to analyze failure in pipeline exposed to significant landslide displacement. This approach has been previously used for dent integrity management. Critical strain is a key material property in this

https://doi.org/10.52202/078572-0019

methodology, and consequently allows weld, HAZ and base metal ductility characterization. This strain corrected for triaxiality, utilizing critical strain, predicts incipient cracking. The approach begins with a global model, followed by a local submodel. This methodology allows one to represent each element of the pipeline; base metal, weld, HAZ, associated material properties and the effect of volumetric defects, weld misorientation etc. can be modelled and characterized.

PROBLEM BACKGROUND, METHODS, AND MATERIALS

Geohazards (for example landslides, slope movement etc.) cause very high longitudinal strain on a short span of pipeline. This longitudinal strain when superimposed with the weld or material related defect, causes failure or unacceptable operational circumstances. Given the longitudinal strain demand is high, the strain capacity with the presence of girth weld or material defects is severely compromised leading to failure. Therefore, it is critical to first understand the strain demand for a geohazard scenario and then assess the strain capacity of the pipeline. Strain demand can be obtained from the geotechnical displacement, and the resulting longitudinal membrane and bending strains. Strain capacity on the other hand can be obtained from accurate material characteristics for the base metal, weld material and heat affected zone. The section below explains the overall logic for one such failure event. Initially the background of the 36-inch Pipeline failure is described along with the resulting strain demand followed by strain capacity of the pipeline. Finally, the results and discussions elucidate the different scenarios and importance of critical strain-based ductile failure model.

36-inch Pipeline Failure Background

A 36-inch (0.515-inches WT) X70M grade pipeline experienced rupture at a girth weld at an operating pressure of around 1,250 psig. This failure resulted in 165 MMSCF of natural gas and the ejection of approximately 80 ft of pipe from the ditch, and a fire that burned for approximately 1½ hours. The pipeline was pigged using a caliper tool and was also hydrostatically tested at 1,880 psig establishing a MAOP of 1,440 psig. Failure occurred in approximately 6 months after being placed in service. In addition, due to excessive bending, the pipeline buckled 63 ft away downstream of the original parting fracture as illustrated in Figure 1.

Figure 1: Illustration of pipeline failure and buckling

https://doi.org/10.52202/078572-0019

There are indications from the field investigation, laser scan data, and fracture wall thinning that there was large geotechnical lateral displacement of approximately 16.5 ft that have resulted in the failure. Therefore, the overall failure event can be described as a pipeline initially laid straight, got displaced to approximately 16.5 ft and ruptured at a girth weld location (#GW24900), with an observed buckling 63 ft downstream of the rupture event.

Longitudinal Strain Demand

Figure 2 shows the plan view of the girth welds in the vicinity of the failure. The point of failure (i.e., at GW# 24900) is marked as red dot. The red arrows represent the distances after the failure. The bold line represents the constructed layout of 150 ft section of pipeline and confirmed through ILI survey conducted six months earlier. The dashed line approximates the final displaced pipeline after a landslide event with distances measured for two girth weld locations (GW#24880 and #24900). There are five girth welds (GW #24870-910) in the displaced span. The geotechnical displacement due to landslide is along the plane of pipeline layout. Caliper and IMU data prior to rupture gave the initial layout of the pipeline, confirming original layout and circular cross-section throughout the pipe segment. ILI reports conducted earlier on the pipe segment also doesn't report any weld flaws in the 150 ft pipe segment.

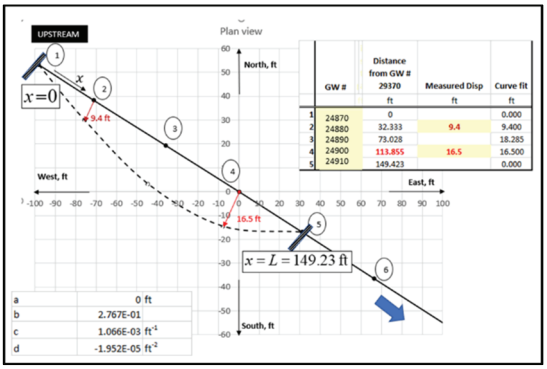

Figure 2: Illustration of the original and displaced view of pipeline

Given the span *L* of the pipe between GW#24870 and GW #24910 is 149.42 ft, the pipeline trajectory was mapped by cubic polynomial:

$$y(x) = a + bx + cx^2 + dx^3 \quad (1)$$

Where x is the distance along the pipe centerline and y is the transverse displacement in ft units. Point of origin is considered at GW#24870. The coefficients are a = 0; b = 0.276; c = 1.066e-3 and d

https://doi.org/10.52202/078572-0019

= -1.952e-5. The trajectory beyond this 150 ft section follows the initial pipeline layout. The elongation of the pipe centerline due to the transverse displacement can be calculated as

$$\Delta L = \int_{x=0}^{L} \sqrt{1 + \left(\frac{dy}{dx}\right)^2}\,.\,dx - L \approx \frac{1}{2}\int_{x=0}^{L} \left(\frac{dy}{dx}\right)^2 .\,dx \quad (2)$$

By substituting Eq. (1) into Eq. (2), the mean axial strain of the pipe centerline can be obtained, i.e.

$$\frac{\Delta L}{L} = b^2 + \frac{4c^2L^2}{3} + \frac{9d^2L^4}{5} + 2bcL + 3cdL^3 + 2bdL^2 \quad (3)$$

With the values of polynomial coefficients, the mean axial strain is 4.56% (> 0.5% yield strain). This implies that the entire cross-section of the pipeline (between GW#24870 and GW#24910) is above yield strain or the membrane strain is way above yield strain.

The next question relates to obtaining the bending strain of the pipeline. The bending strain can be computed from the curvature of the pipeline trajectory. The curvature of the pipeline (κ) at the point of failure is obtained and is given by.

$$\kappa = \left|\frac{d^2y}{dx^2}\right|_{x=113.85} = 0.01121_{\text{ft}^{-1}} \quad (4)$$

Bending strain can be obtained by $\kappa.OD/2$ and is equal to 0.016 or 1.6%, which is again above the yield strain. The radius of curvature ($1/\kappa$) of the entire pipeline segment is illustrated in Figure 3. The figure shows that the radius of curvature of the entire pipe span is below the radius of curvature required to initiate yielding at the pipe OD.

This implies that the entire pipe span was yielded. Radius of curvature to initiate yielding at Pipe OD can be calculated by bending stress equation and then equating it to the yield stress as:

$$\sigma_b = \frac{My}{I} = \frac{(EI\kappa)y_{na}}{I}$$

$$\sigma_b = \sigma_y = \frac{Ey}{R} \quad (5\text{ a, b})$$

where, σ_b and σ_y is the bending stress and yield stress respectively. *I* is the second moment of inertia and y_{na} is the distance from the neutral axis and will be equal to OD/2 for this situation.

https://doi.org/10.52202/078572-0019

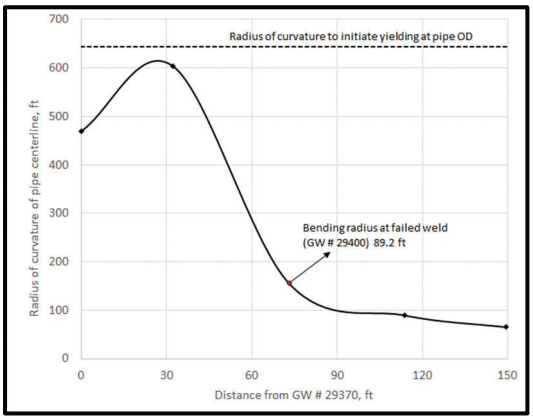

Figure 3: Radius of curvature of the pipeline span with the geotechnical displacement

Assessment Methods: Limit State Calculation

Once the longitudinal strain demand is known, the next step is to assess whether the pipeline can sustain such large geotechnical displacement. In addition, the pipeline segment was operating at an applied pressure ranging from 1240 to 1280 psi. Large displacement caused due to landslide induced high axial tension as described above, thereby inducing a biaxial stress state. The ductile rupture limit of pipelines under such combined loading (i.e., pressure and axial tension) can be obtained using the limit state approaches. Klever-Stewart ductile rupture limit state can be used to obtain the limit state of a 36 in. OD × 0.515 in. 70 ksi pipeline as shown in Figure 4. The *y*-axis represents the differential pressure on the pipeline, i.e. the internal pressure minus the external pressure. The *x*-axis represents the effective force on the pipeline. The effective force is defined as

$$F_{eff} = F_{axial} - P_i A_i + P_o A_o \quad (6)$$

where F_{eff} is the effective force, F_{axial} is the axial force applied on the pipeline, and P_i and P_o represent the internal and external pressures. A_i and A_o represent the internal and external areas of the pipe. The envelope in Figure 4 has been drawn by assuming the external pressure as zero.

The region enclosed by the solid black line and the dashed black line represents the range of internal pressures and axial forces that the pipe can withstand without structural rupture. The dashed line represents the region where the combination of pressure and tension can cause structural failure by necking. The light-yellow band shows the range of operating pressures in the pipeline. From the pipe geometry, and the load required to initiate necking, the strain to initiate necking is 0.36%. The region above the 0.36% mark (i.e., red dot on Figure 4.) represents the rupture and below the mark

https://doi.org/10.52202/078572-0019

represents necking due to axial elongation. Recall from the previous section, that mean axial strain due to the elongation was about 4.56%. The strain and the pressures show that the rupture limit can be exceeded.

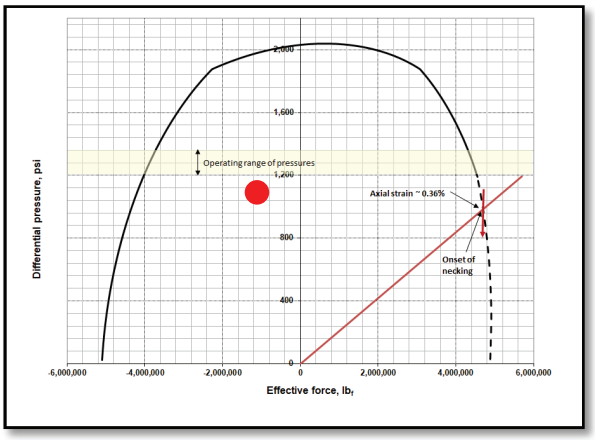

Figure 4: The ISO 10400 ductile rupture limit state of the 36 in. x 0.515 in. 70 ksi pipe (85 ksi ultimate strength)

Above the limit state suggests that the response of the pipeline to such combined loading is unacceptable for continued operation. Ground movement or other unusual upsetting events as in this case exposes the pipeline to high longitudinal strain. For such loading conditions, the traditional stress-based design and assessment methods are usually not suitable as also observed from the approach above. Therefore, it is essential to understand the strain-based damage to explain the geotechnical strain pipeline failure. Following sections discuss a critical strain-based damage methodology to further analyze the problem and assess the impact of girth weld with the large displacement due to landslide.

Critical Strain Based Ductile Failure Methodology

Strain based approaches take advantage of the behavior characteristics of the pipe materials and allow the pipeline to deform until a certain critical strain limit (irreversible cracking tendency). Large plastic deformation of ductile materials involves initiation, growth, and coalescence of microvoids to cracks as illustrated in Figure 5. Microvoids initiate after some significant displacement and continue to form and coalesce, then crack. Incorporating the local plasticity and the stress triaxiality, strain damage models are used to determine the onset of cracking or the point where the structure can't have sufficient strength to functionally operate.

https://doi.org/10.52202/078572-0019

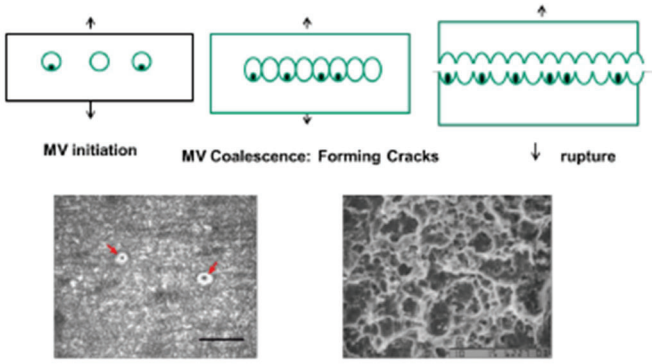

Figure 5: Illustration of void coalescence and failure methodology leading to strain based ductile rupture methodology

The approach is based on two concepts- *Critical Strain,* a material property (ε_o) that is the limit for damage accumulation, and a *Ductile Failure Damage Indicator (DFDI),* a parameter that accumulates with the geotechnical damage. DFDI is a continuum damage mechanics parameter derived from the concept of initiation, growth, and coalescence of voids on a macro scale and formation of cracks with post-yield deformation for a ductile material. Hancock and Mackenzie (1976) in the mid-1970s followed Rice et al.'s (1969) [10, 11] work and proposed a reference failure strain, ε_f, i.e., a strain limit for ductile failure as a function of mean stress,σ_m, and equivalent stress, σ_{eq}:

$$\varepsilon_f = 1.65\varepsilon_o \, exp\left(-\frac{3}{2}\frac{\sigma_m}{\sigma_{eq}}\right) \tag{7}$$

This reference failure strain is used to compute the accumulated damage with the applied displacement and is given as follows:

$$D_i = DFDI = \int_0^{\varepsilon_{eq}} \frac{d\varepsilon_{eq}}{\varepsilon_f} = \frac{1}{1.65\varepsilon_0}\int_0^{\varepsilon_{eq}} exp\left(\frac{3}{2}\frac{\sigma_m}{\sigma_{eq}}\right) d\varepsilon_{eq} \tag{8}$$

Incremental plastic strain ($d\varepsilon_{eq}$) were accumulated with geotechnical displacement. When the total strain is integrated as the pipeline is displaced and it equals the failure strain limit at which point the plastic damage transforms into a crack. DFDI value ranges from 0 (undamaged) to 1 (crack). By definition, ductile failure or failure of a structural body will occur when D ≥ 1.

This method tends to capture different material responses corresponding to weld, HAZ and base metal, along with the traixiality of loading [12]. Note that the geotechnical displacement loading is a biaxial loading state and therefore, it is essential to capture the triaxiality in predicting the damage.

https://doi.org/10.52202/078572-0019

Pipeline Failure Finite Element Modeling

The finite element approach is suited to illustrate the failure mechanism of the pipeline subjected to the large lateral geotechnical displacement. Lateral displacement of the pipeline was modeled in ABAQUS using a global-local sub modeling approach. According to the global-local submodeling approach, a global model of large domain (i.e., 149 ft in this case) is modelled showing the global strains on the pipeline segment. Then a smaller submodel of 100-inches is modelled with loads from the global model to capture the local details. The pipeline segment of roughly 149 ft. was modelled as a 3-D beam in ABAQUS. Element size of 1 in. was used to mesh the global model. 36 in. OD and a wall thickness of 0.515 in. was assumed for the pipe cross-section. Figure 6 illustrates the schematic of the global model along with the applied end conditions. The two ends of the pipeline segment were excavated from the ground. The ends were not laterally displaced from the construction location. Simply supported end conditions were therefore assumed at the ends. Rotation at the ends is permitted.

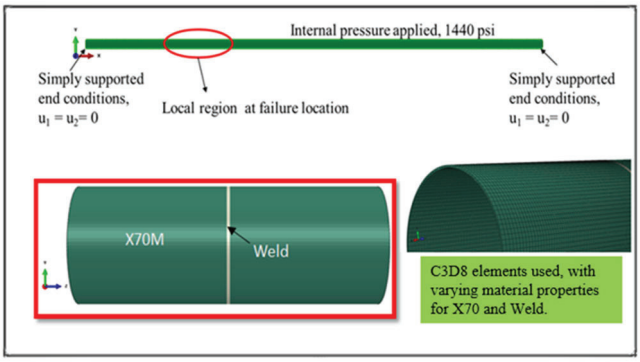

Figure 6: Illustration of global and local submodeling approach. 149 ft of global pipeline along with 100-inch of local submodel

Later a detailed although much smaller submodel with weld and base material is modelled. The weld geometry is not modelled specifically, but instead the submodel geometry in the Figure 6 uses material properties specific to base material and weld. The severity of the GW is accessed using the stresses, strains, and by ductile failure damage indicator (DFDI). Several pull-to-failure tensile tests were conducted on pipe and weld material from the ruptured pipe segment to obtain the material characteristics of base material and weld metal. Figure 7 shows the engineering and true stress-strain responses of the base material (X70 steel grade) and weld.

The true strain of failure for the base material and weld metal is 125% and 65%, respectively obtained directly from the hi-resolution diameter measurements as explained in detail by Gao et. al., 2013 [13]. Critical strain, an important variable to monitor the damage accumulation was obtained for weld material and X70 steel material. Material properties of the X70 and weld, used for the FE modeling, are listed in Table 1. A typical Young's modulus and Poisson's ratio of 30,000 ksi and 0.3,

https://doi.org/10.52202/078572-0019

respectively, were used in the analysis. A very important parameter to note is that the critical strain of weld material is approximately half of the X70 material as also observed from the true failure strain in Figure 7. Therefore, with same loading the accumulated damage will be twice the magnitude for the weld compared to the base material. In addition, the geometry of weld along with the loading will introduce the triaxial stress state which would be captured by ductile damage failure model (DFDI). Comprehensive modeling details and the failure analysis discussion is included in the section below.

Table 1: Summary of material properties used in FEA

Material Properties	X70	Weld Material
Modulus of Elasticity (ksi)	30,000	30,000
Poisson's ratio	0.3	0.3
Critical Strain	0.59	0.32
Yield Strength (ksi)	79.4	70.8

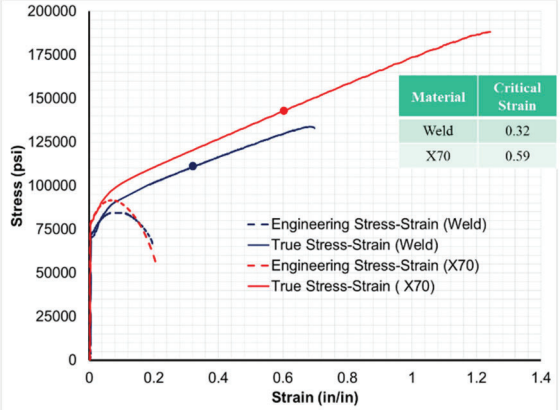

Figure 7: Engineering and true stress-strain behavior of weld and base pipeline material

FAILURE ANALYSIS RESULTS AND DISCUSSION

36-inch. pipeline subjected to large displacements would develop large strains caused by elongation and bending as illustrated above. However, the material characteristics can provide an estimate of local damage that would initiate microcracks and then finally to failure as explained in detail by Gao et. al., 2013 [13]. In addition, the damage can be aggravated due to local weld misalignment or weld imperfections. Strain damage models are used to determine the onset of cracking due to local plasticity. Sections below discuss the process of failure mechanism of the pipeline in steps.

https://doi.org/10.52202/078572-0019

Large Displacement Pipeline Strain Capacity

As shown in

Figure 2 the pipeline section between girth weld #24870 and #24910 experienced a large lateral displacement normal to the pipe centerline. In addition, a sample containing the "buckle" was two girth welds downstream of GW # 24910 and excavated from under nearly 15.3 ft. of the earth. Based on these observations it is reasonable to assume a "lateral restraint" on the pipeline upstream of weld #24870 and downstream of Weld #24910. The displacement profile per the curve fitting as shown in

Figure 2 was applied to the 3-D global beam model, whilst the ends were restrained in simply supported conditions. The internal pressure of 1440 psi was also applied on the ID surface of the pipeline. As the displacements are large, the internal pressure has very little to no effect on the final failure.

Global reactions, stresses and strains were obtained from the global model. Also, sectional forces and moments were obtained at the failure location (Weld # 24900) as shown in Figure 8 which were then applied on the ends of the local sub-model. Figure 8 shows the sectional forces and moment distribution as a function of the applied displacement at the GW 24900. The final values, axial load of 5755 klb_f and a moment of 2815 klb_f–in, at a displacement of 16.5 feet were applied on the sub model.

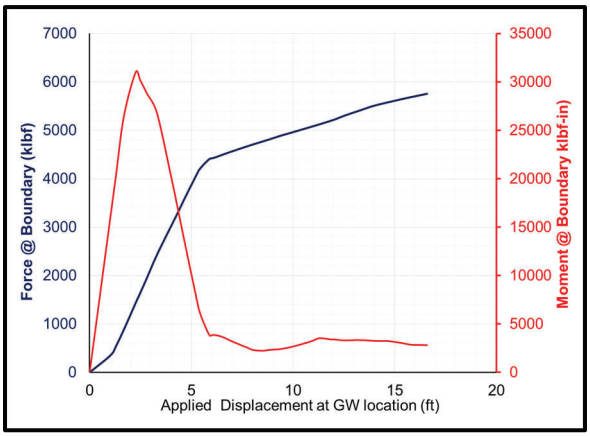

Figure 8: Section forces and moment obtained from the global model at the GW location or point of failure

Deflection, stresses, and strains as obtained from the global model are illustrated in Figure 9 below. The axial stress of around 101 ksi is observed at the GW location. Effective plastic strain of around 9.1% is observed at the girth weld cross-section. Stresses and strains are high at the GW location, but

https://doi.org/10.52202/078572-0019

not significant enough to cause rupture. This conclusion is based on the global model; the weld details are captured in the local sub-model.

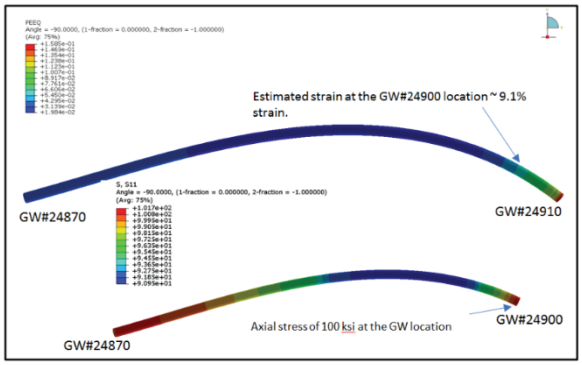

Figure 9: Effective plastic strain and axial stress along the pipe segment. Plastic strain of 9.1% observed at the failure location

In addition, the global moment illustrated in Figure 8 shows an increase followed by decrease after 2.5 ft of displacement. This also indicates that the pipeline segment buckled losing its strength following which the damage at the girth weld is primarily a function of increased axial stress (bending and membrane), which can be captured with local submodel results.

Local Damage and Strain Capacity at the weld

Global strain as illustrated above is under the strain capacity of the pipeline. Normally the pipeline would sustain such high strain in absence of girth weld or weld related defects. Subsequently, it is essential to understand the strain capacity of girth welds through local or submodeling approach.

Two different sub-models were considered:

- Weld and base metal have the same X70M properties.
- Weld has weld properties and base metal has X70M properties.

The results of the modeling are shown in Figure 10 with the maximum principal stresses and strain distribution on the sub-model at the maximum displacement of 16.5 feet along with internal pressure. Immediately it is evident that with the weld properties being different than the base metal exhibits higher total strains (15% compared to 8.6%).

https://doi.org/10.52202/078572-0019

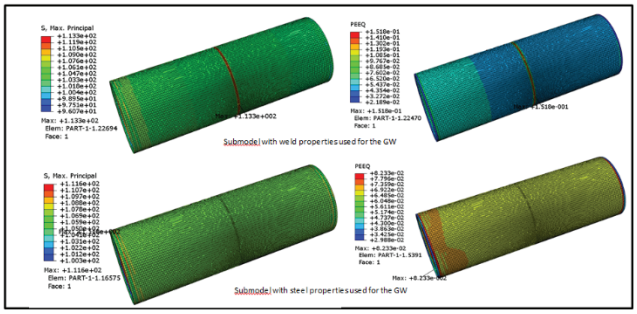

Figure 10: Maximum principal stress and plastic strain for the submodels

To assess whether the weld would fail one has to start reviewing the DFDI. Figure 11 and Figure 12 shows the DFDI distribution for the two cases; it approaches 0.45 when the properties are uniform across the weld, however it is 0.86 when the weld and base metal have their measured properties. As discussed previously, DFDI or accumulated damage should be 1.0 before the localized plasticity can turn the voids into a microcrack. This implies that the pipeline with perfectly aligned weld and no weld imperfections would sustain at 16.5 feet of lateral displacement.

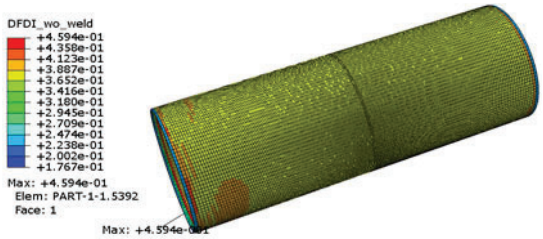

Figure 11: Illustration of DFDI for the submodel with base metal properties for girth weld

The analysis also showed that failure will occur (or DFDI would be above 1.0) for the pipe segment at an approximate displacement of around 18 feet of displacement at GW 24900.

https://doi.org/10.52202/078572-0019

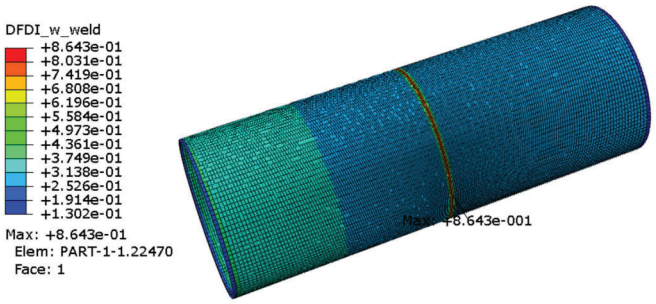

Figure 12: Illustration of DFDI for the submodel with weld properties for girth weld

Strain Capacity with Weld Misalignment Effects

The affected segment of the Pipeline was constructed using API Specification 5L (45th Edition) Grade X70M PSL2 line pipe and fittings (0.515-inch pipeline section, and 0.618-inch-thick fittings), which were joined end-to-end in the field by welders using the shielded metal arc welding (SMAW) process. Small misalignment (hi-lo) was observed in the weld samples. Based upon measurements made on Weld No. 24900, misalignment was determined to range from about 1 to 2 mm; therefore, it was decided to model a misalignment of 1.25mm (0.05 in.) at Weld # 24900. The left end of the pipe segment in the sub-model was shifted down by 0.05 inches to create the misalignment (as shown in Figure 13). Sub-model was analyzed by considering section forces and moments obtained from the global model and applied on ends.

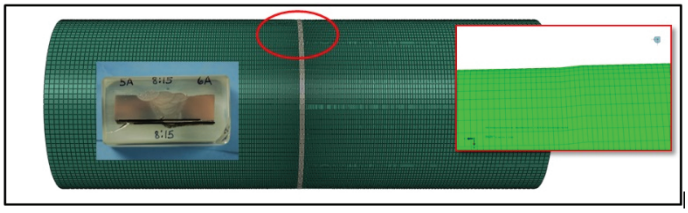

Figure 13: Illustration of 1.25 mm weld misalignment modeled in weld geometry submodel

Figure 14 shows the accumulated damage distribution on the sub-model. It is observed that the local model with misalignment has accumulated damage of more than 1.0 at an applied axial load of 5610 klbf or lateral displacement of 15.26 feet. The maximum principal stress of 124 ksi and an equivalent plastic strain of 32% is observed at the GW location. The critical strain of the weld material is approximately 32%, which suggests that the lateral displacement will induce high strains leading to pipe cracking. Based on this model the weld is predicted to fail or rupture at a displacement of 15.26 feet.

https://doi.org/10.52202/078572-0019

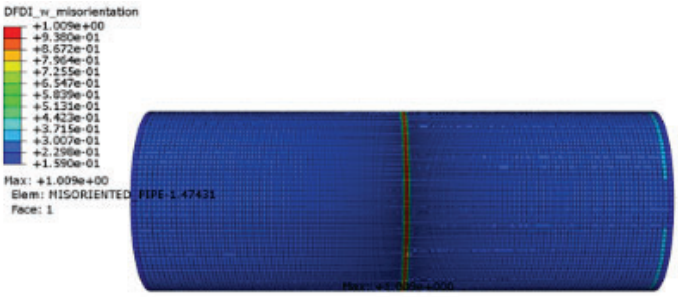

Figure 14: Illustration of DFDI for the weld misaligned submodel

Strain Capacity with Weld Anomalies

According to API 1104 there are imperfections that are allowable; despite being an allowable imperfection these will cause local strains during the large displacement event. Consequently, a planar imperfection (allowable by API 1104) was assessed in the sub-model. A planar imperfection of 1" (L), 1/8" (D) and 1/16" (W) with an elliptical cross-section along with the misorientation of 1.25 mm (0.05") were introduced into the girth weld of the sub-model. Again, using the weld and X70 steel grade properties, the model as illustrated in Figure 15 was analyzed with the section forces and moments from the global model.

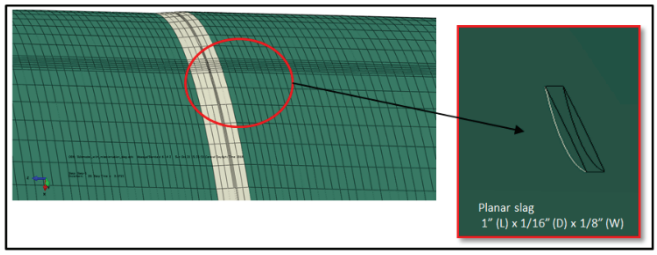

Figure 15: Illustration of elliptical planar slag along with GW misorientation in the sub-model

Figure 16 shows the maximum principal stress, equivalent plastic strain (PEEQ) and accumulated damage distribution on the sub-model. It is observed that the local model with misorientation has accumulated damage (DFDI) of more than 1.0 at an applied axial load of 5480 klbf or an applied lateral displacement of 13.76 feet. Maximum principal stress of 161 ksi and an equivalent strain of 24% is observed at the tip of the planar imperfection. The weld with the allowable defect and weld misalignment will fail at an applied displacement of 13.76 feet rather than 16.5 feet in the absence of the imperfection.

https://doi.org/10.52202/078572-0019

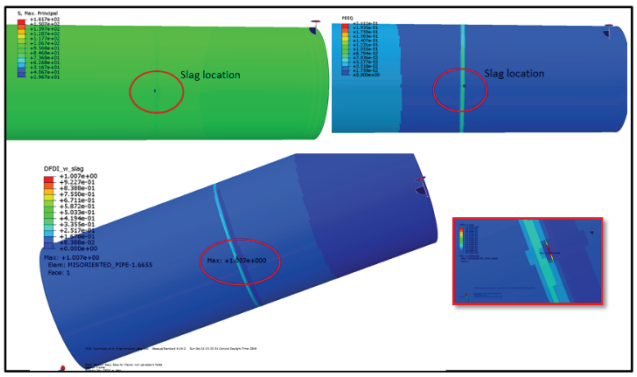

Figure 16: Maximum principal Stress (ksi), strain and accumulated damage (DFDI) distribution on the sub-model with planar imperfection.

Based on the finite element model and the measured properties of the weld, the pipeline could have failed when the pipeline displaced 13.76 to 15.26 feet. The exact allowable imperfections in the failed weld are unknown; since the weld misalignment is known to exist in this weld the failure appears to have occurred when the pipeline was displaced between 13.76 to 15.26 feet. The ductile failure, consistent with the laboratory analyses, is predicted to occur at the displacements measured in the field.

Buckling Discussion

This Pipeline segment also showed buckling at the GW 24920 (Figure 1, also the restrained end) location. Pipe segment subjected to soil movement may induce bending, combined with axial elongation and internal pressure while in operation. A pipe subjected to bending may also fail due to local buckling. Buckling on the pipeline segment is analyzed by considering soil movement that may cause the pipe to bend. This bending with one constrained end would cause buckling.

Pipe, when bent about its longitudinal axis, will lose its elastic stability at some applied moment, and could buckle. Pipe samples were excavated with a 15.3 ft. depth of cover after the incident and showed buckled. The orientation of the buckle is approximately 90° clockwise from the 12 o' clock position of the pipeline. The pipe segment loses its strength and stability with buckling and forms a hinge at the point of buckling. Buckling response, "Moment (M) - Curvature (κ)," depends upon the Moment of Inertia of the pipe, Yield strength of the material, Internal pressure applied on the pipe, Axial load applied on pipe.

The point of elastic instability is obtained through a series of FEA analyses on the pipe segment. Pipe segment with 36 in. OD and 0.515 in. wall thickness were subjected to pure bending, with varying

https://doi.org/10.52202/078572-0019

axial load and pressure. Pipe segment was modeled with shell elements (i.e., S4R) and the point of elastic instability is illustrated through Moment (M) - Curvature (κ) responses as shown in Figure 18.

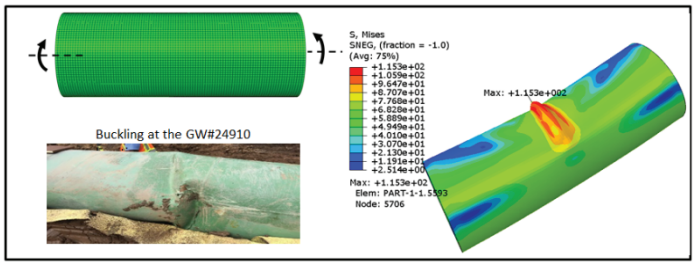

Figure 17: Illustration of pure bending applied to the pipeline segment. The buckled sample as obtained from the failure site is also shown for comparison.

Point of elastic instability was established with a series of finite element models with varying axial loads and pressures on a pipe segment subjected to pure bending. Elastic instability with combined loading (internal pressure, bending and axial load) is also influenced by the elastic-plastic material properties and occurs when the entire pipeline cross-section has yielded. Moment (M)-Curvature (κ) response of the pipe segment using the X70 material properties and combined loading is obtained and shown in Figure 18. Point of elastic instability for a pipeline subjected to pure bending is given by:

$$M_p = 4\sigma_y r_0^2 t \qquad (22)$$

where σ_y is the yield strength, r_0 is the outer radius of pipeline and t is wall thickness.

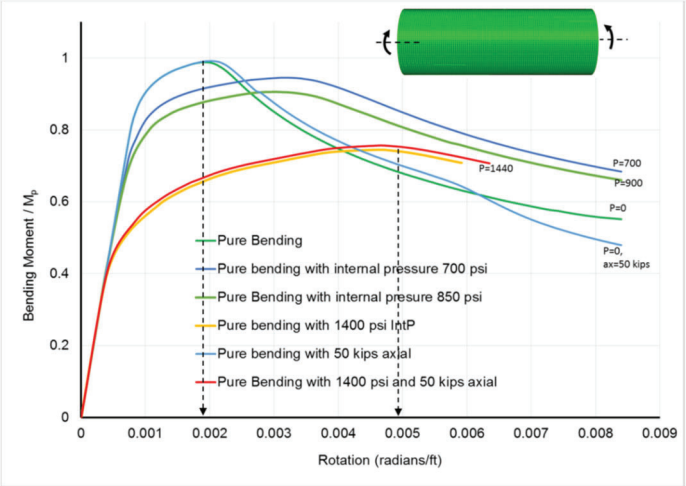

Figure 18: Moment (M)-Curvature (κ) responses for a pipe segment subjected to combined loading

Figure 18 shows the moment curvature response for the pipe segment with X70 material properties and 36 in. OD and 0.515 in. WT and an internal pressure ranging from 0 to 1440 psi. As shown in Figure 18, the moment starts dropping with continued rotation at the center of the pipe. This point

https://doi.org/10.52202/078572-0019

is the point of buckle and that occurs at an applied curvature of 0.005 rad/ft. This provides the curvature at Weld No. 24920 that would cause buckling.

Lateral displacement of the pipeline segment will introduce bending that could lead to buckling. Angular rotation or curvature can be translated to equivalent lateral displacement. Lateral displacement of approximately 9.93 ft at Weld #24900 (failure location) would result in a local curvature of 0.005 rad/ft at Weld #24920. Therefore, it can be assumed that the pipeline buckled after a displacement of 9.93 ft leading to loss of elastic stability at the buckled location. However, the pipeline continued with further lateral displacement until the ductile failure limit of the weld was reached at Weld #24900.

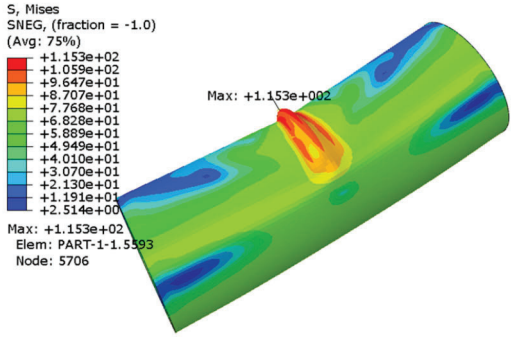

Figure 19: Illustration of buckling by applying bending or rotation about the central axis

CONCLUSION

The Pipeline rupture was caused by a large lateral displacement, where the pipeline was displaced by 16.5 ft at failure event. Overloading of the pipeline resulted from what was likely a series of lateral displacements with accompanying bending.

The strain-based approach that utilized critical strain as a material property and DFDI as a damage parameter quantitatively predicted the displacement at which the pipeline would fail. Finite element modeling illustrated that the damage accumulated to critical levels for fracture of Weld No. 24900 could not be attained (with perfectly aligned pipes) prior to displacement of this weld having reached 18 feet. However, introduction of internal misalignment (hi-lo condition) of 1.2 mm (0.049 inch) resulting in predicted failure of Weld No. 24900 after a displacement of only 15.26 feet (minimum).

With a weld imperfection (elongated slag inclusion), which is acceptable under API 1104 rules the displacement required to cause failure of Weld 24900 decreased from 15.26 to 13.76 feet. In addition, the pipeline buckled prior to the failure event and approximately when the displacement at Weld No. 24900 had reached 9.93 feet. Thus, the failure of Weld 24900 was caused primarily by the effects of a large lateral displacement and was assisted by the effects of weld material

https://doi.org/10.52202/078572-0019

characteristics, which concentrated strains in the root area of the weld, and by hi-lo that further increases damage.

Since DFDI indicates the onset of crack incipient, it would be more appropriate for large displacement strain-based engineering assessments. Synergistic interplay of the geotechnical displacement along with weld misalignment and weld defects reduces the strain capacity thereby leading to several geohazard pipeline failures, and that was successfully modeled using the critical strain-based damage methodology. The physical micro-mechanical strain-based failure model as outlined in this work can be utilized for pipeline design for geohazards and other large displacement incidents with appropriate safety factor that accounts for material variability and allowable defects, if any.

ACKNOWLEDGMENTS

Authors would like to thank TC Energy for providing the support in conducting the failure analysis of a 36-in. failure due to slope movement and Blade Laboratories to obtain the material characterization curves for weld and base metal.

REFERENCES

[1] G. Wu and L. Wang, "An Overview of Strain Based Fracture Assessment of Pipelines," in *International Conference on Ocean, Offshore and Arctic Engineering, OMAE2018*, Madrid, 2018.

[2] "CSA Standard Z662-23: Oil and Gas Pipeline Systems, Canadian Standards Association," Canadian Standards Association (CSA), Mississauga, Ontario, Canada, 2023.

[3] D. P. Fairchild, S. Kibey, H. Tang, V. Krishnan, X. Wang, M. Macia and W. Cheng, "Continued Advancements regarding Capacity Prediction of Strain based Pipelines," in *Proceedings of 9th International Pipeline Conference*, Calgary, 2012.

[4] Y.-Y. Wang, M. Liu, F. Zhang, D. Horsley and S. Nanney, "Multi-Tier Tensile Strain Models for Strain Based Design Part-1 Fundamental Basis," in *9th International Pipeline Conference*, Calgary, 2012.

[5] M. Liu, Y.-Y. Wang, Y. Song, D. Horsley and S. Nanney, "Multi-Tier Tensile Strain Models for Strain Based Design Part 2- Development and Formulation of Tensile Strain Capacity," in *9th International Pipeline Conference*, Calgary, 2012.

[6] Y.-Y. Wang, M. Liu, Y. Song, M. Stephens, R. Petersen and R. Gordon, "Second Generation Models for Strain-Based Design," PRCI- DTPH56-06-T000014, 2011.

https://doi.org/10.52202/078572-0019

[7] H. Tang, D. Fairchild, M. Panico, J. Crapps and W. Cheng, "Strain capacity prediction of strain-based pipelines," in *10th International Pipeline Conference*, 2014.

[8] A. Fredj, "Pipeline Response to Slope Movement and Evaluation of Pipeline Strain Demand," in *10th International Pipeline Conference, IPC2014*, Calgary, 2014.

[9] L. Ming, Y.-Y. Wang, F. Zhang and K. Kotian, "Realistic Strain Capacity Models for Pipeline Construction and Maintenance," DTPH56-10-T-000016, USDOT- PHMSA, 2013.

[10] J. W. Hancock and A. C. McKenzie, "On the mechanisms of ductile failure in high-strength steels subjected to multi-axial stress-states," *J of Mechanics and Physics of Solids,* vol. 24, pp. 147-169, 1976.

[11] "Rice, J; Tracey, D," *On the ductile enlargement of voids in tri-axial stress fields,* vol. Journal of Mechanics and Physics of Solids, pp. 201-217, 1969.

[12] U. Arumugam, M. Gao, R. Krishnamurthy, R. Wang and R. Kania, "Study of a Plastic Strain Limit Damage Criterion for Pipeline Mechanical Damage Using FEA and Full-Scale Denting Tests," in *11th International Pipeline Conference*, Calgary, 2016.

[13] M. Gao, R. Krishnamurthy, S. Tandon and U. Arumugam, "Critical Strain Based Ductile Damage Criterion and its Application to Mechanical Damage in Pipelines," in *13th International Conference on Fracture*, Beijing, China, 2013.

[14] M. Gao and R. Krishnamurthy, "Mechanical Damage in Pipelines: A Review of the Methods and Improvements in Characterization, Evaluation, and Mitigation," in *Oil and Gas Pipelines: Integrity and Safety Handbook, R. Winston Revie Ed. , Chapter 22*, Wiley, 2015.

[15] M. Hetenyi, "Beams on Elastic Foundation," Univ. of Michigan Press, 1946, pp. 144-146.

https://doi.org/10.52202/078572-0019